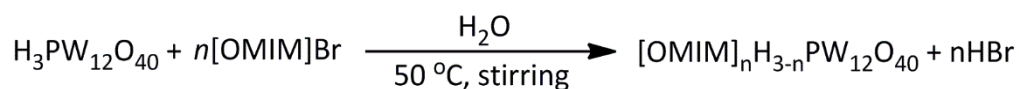


## 1. Experimental Procedures

**Materials.** Ethanol (A. R. grade), acetone (A. R. grade), cyclohexane (A. R. grade) were provided by Sinopharm Chemical Reagent Co., Ltd. Hydrogen (99.99%) and nitrogen (99.99%) was supplied by Beijing Analytical Instrumental Company. Dichloromethane ( $\text{CH}_2\text{Cl}_2$ , 99.5%), cyclohexane (99.5%), cyclohexanone (99.5%) were obtained from the Beijing Chemical Company. Diphenyl ether (99%), 2-Cyclohexylcyclohexanone (97%), palladium acetate ( $\text{Pd}(\text{OAc})_2$ , 98%), 1-methyl-4-phenoxybenzene (95%) 4-phenoxyphenol (99%), *p*-tolyl ether (99%), 4,4'-dihydroxydiphenyl ether (98%) 4-methylcyclohexanone (98%), phenetole (99%), *n*-butyl phenyl ether (99%) and ruthenium (III) chloride (99%) were supplied by J & K Scientific Ltd. *n*-dodecane (99%) and phosphotungstic acid ( $\text{H}_3\text{PW}_{12}\text{O}_{40} \cdot n\text{H}_2\text{O}$ , A.R.), bis(4-methoxyphenyl) ether (98%) and L-lysine (98%) were purchased from Beijing InnoChem Science & Technology Co., Ltd. Potassium bromide (KBr, 99.9%) was purchased from Adamas Reagent. Anisole (99%), cyclohexanol (99%), phenol (99%), Pd/C (5 wt.% Pd) and silicon oxide ( $\text{SiO}_2$ , amorphous) were purchased from Alfa Aesar. Ru/C (5 wt.% Ru), Pd/ $\text{Al}_2\text{O}_3$  (5 wt.% Pd) was supplied by TCI (Shanghai) Development Co., Ltd. Ionic liquids (ILs) including 1-Octyl-3-methylimidazolium bromide ([OMIM] Br, purity>99%) and  $[\text{SO}_3\text{HBMIM}]\text{CF}_3\text{COO}$  (purity>99%) was purchased from the Centre of Green Chemistry and Catalysis, LICP, CAS. Prior to use, the IL was dried *in vacuo* at 80 °C for 24 h.

### 1.1 Catalyst synthesis and characterization

**Synthesis of POM-IL complexes ( $[\text{OMIM}]_x\text{H}_{3-x}\text{PW}_{12}\text{O}_{40}$ ).** The POM-IL complexes including  $[\text{OMIM}]\text{H}_2\text{PW}_{12}\text{O}_{40}$  ( $\text{H}_2[\text{POM-IL}]$ ),  $[\text{OMIM}]_2\text{HPW}_{12}\text{O}_{40}$  ( $\text{H}[\text{POM-IL}]$ ) and  $[\text{OMIM}]_3\text{PW}_{12}\text{O}_{40}$  ( $[\text{POM-IL}]$ ) were synthesized *via* the cation-exchange reaction between polyoxometalate ( $\text{H}_3\text{PW}_{12}\text{O}_{40} \cdot n\text{H}_2\text{O}$ ) and IL ([OMIM] Br), as highlighted in Scheme S1. For the synthesis of  $\text{H}_2[\text{POM-IL}]$ , phosphotungstic acid ( $\text{H}_3\text{PW}_{12}\text{O}_{40} \cdot n\text{H}_2\text{O}$ , 1 mmol) was dissolved in distilled water (60 mL) in a 250 mL round bottom flask, and to this, an aqueous solution of [BMIM] Br (1 mmol in 60 mL  $\text{H}_2\text{O}$ ) was added dropwise at 50 °C with vigorous stirring. Then the mixture was kept stirring at 50 °C for 3 h and white precipitates were generated. Subsequently, the white precipitates which are water-insoluble were separated by centrifugation and washed with distilled water, before drying *in vacuo* at 60 °C for 24 h to afford  $\text{H}_2[\text{POM-IL}]$  as free-flowing powders.  $\text{H}[\text{POM-IL}]$  and  $[\text{POM-IL}]$  were synthesized in a similar manner, the difference is the amount of employed [OMIM] Br. For these two, the molar ratios of  $\text{H}_3\text{PW}_{12}\text{O}_{40} \cdot n\text{H}_2\text{O}$  and [OMIM] Br are 1:2 and 1:3, respectively.



**Scheme S1.** Cation exchange reaction between  $\text{H}_3\text{PW}_{12}\text{O}_{40}$  and [OMIM]Br.

**Synthesis of silica supported POM-IL complexes ([OMIM]<sub>x</sub>H<sub>3-x</sub>PW<sub>12</sub>O<sub>40</sub>@SiO<sub>2</sub>).** The procedures to synthesize H<sub>2</sub>[POM-IL]@SiO<sub>2</sub> is described here as an example, as that for the synthesis of H[POM-IL]@SiO<sub>2</sub> and [POM-IL]@SiO<sub>2</sub> are similar. The difference is H[POM-IL] and [POM-IL] are used as precursors, respectively. To an acetone solution (100 mL) of H<sub>2</sub>[POM-IL] (0.3 mmol), SiO<sub>2</sub> (3 g, Silica Gel) was added. The dispersion was stirred for 10 minutes in a 250 mL beaker, followed by solvent removal under reduced pressure using a rotary evaporator. Then a fresh portion of acetone (50 mL) was added and the stirring/solvent removal procedure was repeated three times, to achieve uniform dispersion of H<sub>2</sub>[POM-IL] on the SiO<sub>2</sub> surface. Subsequently the obtained material was dried *in vacuo* at 60 °C for 24 h, affording H<sub>2</sub>[POM-IL]@SiO<sub>2</sub> as white, solid, free-flowing powders.

**Synthesis of Pd/POM-IL@SiO<sub>2</sub> (Pd/[OMIM]<sub>x</sub>H<sub>3-x</sub>PW<sub>12</sub>O<sub>40</sub>@SiO<sub>2</sub>).** Pd/POM-IL@SiO<sub>2</sub> was prepared via the conventional wet impregnation method. Palladium acetate (Pd(OAc)<sub>2</sub>, 0.211 g, 0.94 mmol) was dissolved in ethanol (50 mL), and to this, an ethanol suspension (50 mL) of Pd/POM-IL@SiO<sub>2</sub> (2 g) was added. Subsequently, an aqueous solution of lysine (0.6 g, 50 mL) was added dropwise to the mixture under vigorous stirring over 30 min. The mixture was kept stirring at room temperature for 12 h. After solvent removal using a rotary evaporator, obtained materials were washed with distilled water and ethanol for several times, and dried *in vacuo* at 60 °C for 24 h. Then the resulting residues were milled and reduced by subjecting to an atmosphere of hydrogen<sub>(gas)</sub> (6 MPa gauge pressure at room temperature) at 160 °C for 6 h, affording Pd/POM-IL@SiO<sub>2</sub> as black, free-flowing powders. For comparison, we also synthesized Pd/SiO<sub>2</sub> in a similar manner to the procedures described above, the only difference is that SiO<sub>2</sub> instead of Pd/POM-IL@SiO<sub>2</sub> was employed as the substrate.

In addition, Ru/H<sub>2</sub>[POM-IL]@SiO<sub>2</sub> was prepared in a similar manner to Pd/H<sub>2</sub>[POM-IL]@SiO<sub>2</sub>, except ruthenium (III) chloride was used as Ru precursor. Pd/SO<sub>3</sub>H[POM-IL]@SiO<sub>2</sub> (i.e., Pd/[SO<sub>3</sub>HBMIM]<sub>3</sub>PW<sub>12</sub>O<sub>40</sub>@SiO<sub>2</sub>), was also synthesized in a similar way to Pd/H<sub>2</sub>[POM-IL]@SiO<sub>2</sub>, except IL [SO<sub>3</sub>HBMIM] CF<sub>3</sub>COO was employed as the IL precursor during the synthesis of POM-IL composite.

## 1.2 Characterization methods

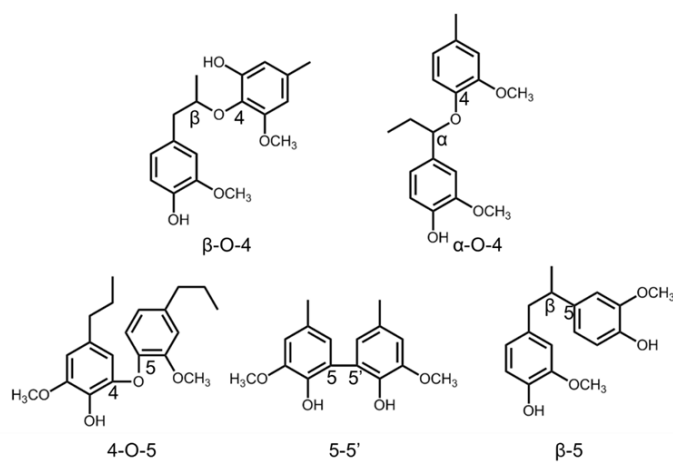
Powder X-ray diffraction (XRD) patterns of the synthesized materials were recorded on a X-ray diffractometer (Model D/MAX2500, Rigaku) with Cu-K $\alpha$  radiation, and the scan speed was 5° min<sup>-1</sup> from 5° to 80°. The scanning electron microscopy (SEM) measurements were conducted on a HITACHI S-4800 Scanning Electron Microscope operated at 15 kV. The samples were spray-coated with a thin layer of platinum before observation. The transmission electron microscopy (TEM) images were obtained using TEM JEOL-1011 and/or JEOL-2100F TEM with an accelerating voltage of 120 kV. The porosity properties of the synthesized materials were obtained from nitrogen adsorption-desorption isotherms using a Micromeritics ASAP 2020 V3.00 H (USA) system. The samples were degassed at 120 °C for at least 12 h before subjected for measurements. X-ray photoelectron spectroscopy (XPS) measurements were carried out on an ESCAL Lab

220i-XL spectrometer at a pressure of  $\sim 3 \times 10^{-9}$  mbar (1 mbar=100 Pa) using Al K $\alpha$  as the excitation source ( $h\nu=1486.6$  eV) and operated at 15 kV and 20 mA. Fourier-transform infrared spectroscopy (FT-IR) analysis of the samples was performed on a Bruker Tensor 27 infrared spectrometer and the samples were diluted with KBr and pressed as a pellet. The contents of Pd in the synthesized materials were determined by ICP-AES (VISTA-MPX). Prior to analysis, samples were acid-digested in HCl and HNO<sub>3</sub> concentrated aqueous solution at a volume ratio of 3:1.

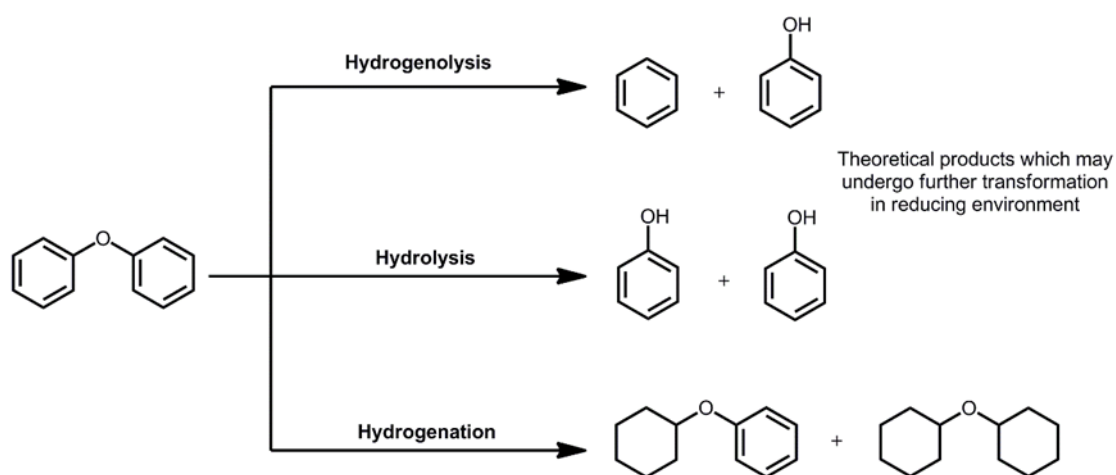
### 1.3 Catalytic reactions

The catalytic reactions were conducted in a Teflon-lined stainless-steel reactor of 20 mL equipped with a magnetic stirrer. In a typical experiment, substrate (1 mmol), water (2 mL) and the catalyst (30 mg) were charged into the reactor. After sealing, the air in the reactor was removed *in vacuo* and the reactor was purged with hydrogen to make sure air is completely removed at room temperature. The hydrogen in the reactor was charged to desired pressure (3 MPa), before subjecting the reactor to a furnace at desired temperature for a known amount of time with a stirring speed of 600 r.p.m. After the reaction, the reactor was cooled in ice-water bath. Products were extracted from the reaction mixture using dichloromethane for three times, prior to which dodecane was added as internal standard. The qualitative analysis of products was achieved by GC-MS (Agilent 5975C-7890A) and compared with authentic samples. Quantitative analysis was conducted using GC (Agilent 7890B) equipped with a flame ionization detector and an HP-5 capillary column (0.32 mm in diameter, 30 m in length) using Argon as the carrier gas. To study reusability, the catalyst was recovered by centrifugation, and washed with distilled water for three times. After drying *in vacuo* at 80 °C for 12 h, the catalyst was reused for the next run. The qualitative and quantitative analysis of reaction products was similar to that mentioned above.

## 2. Results and Discussion

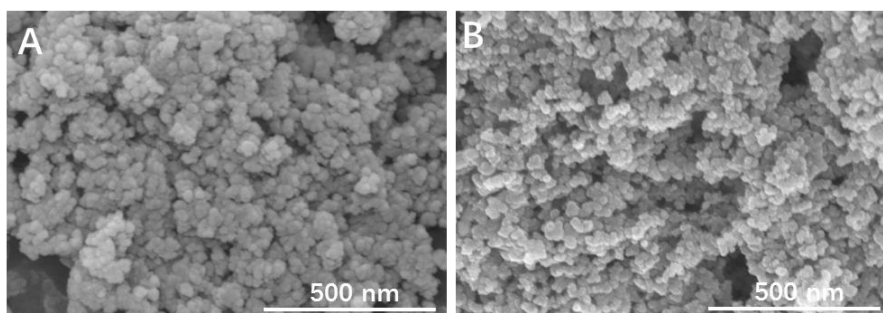


**Figure S1.** Typical linkages in lignin structure.



**Figure S2.** Possible reaction pathways for reductive transformation of diphenyl ether in the presence of hydrogen.

### 2.1 Characterization of synthesized catalysts

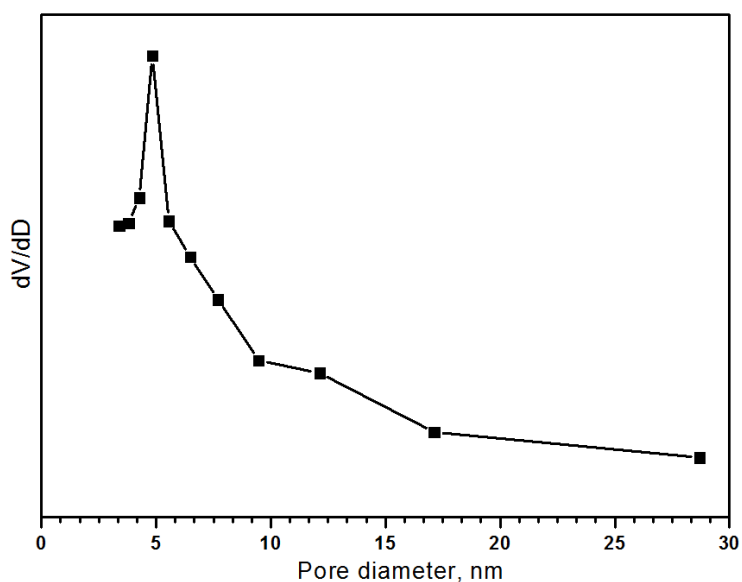


**Figure S3.** SEM images of (A) Pd/H<sub>2</sub>[POM-IL]@SiO<sub>2</sub> and (B) SiO<sub>2</sub>.

**Table S1.** Porosity of SiO<sub>2</sub> and synthesized Pd/POM-IL@SiO<sub>2</sub> and Pd/SiO<sub>2</sub><sup>[a]</sup>

Sample <sup>[b]</sup>	BET surface area (m <sup>2</sup> g <sup>-1</sup> )	Pore volume (cm <sup>3</sup> g <sup>-1</sup> )	Pore diameter (nm)
SiO <sub>2</sub>	156	0.4	4.8
Pd/H <sub>2</sub> [POM-IL]@SiO <sub>2</sub>	94	0.4	3.4
Pd/H[POM-IL]@SiO <sub>2</sub>	87	0.3	3.1
Pd/[POM-IL]@SiO <sub>2</sub>	81	0.3	3.0
Pd @SiO <sub>2</sub>	127	0.3	3.4

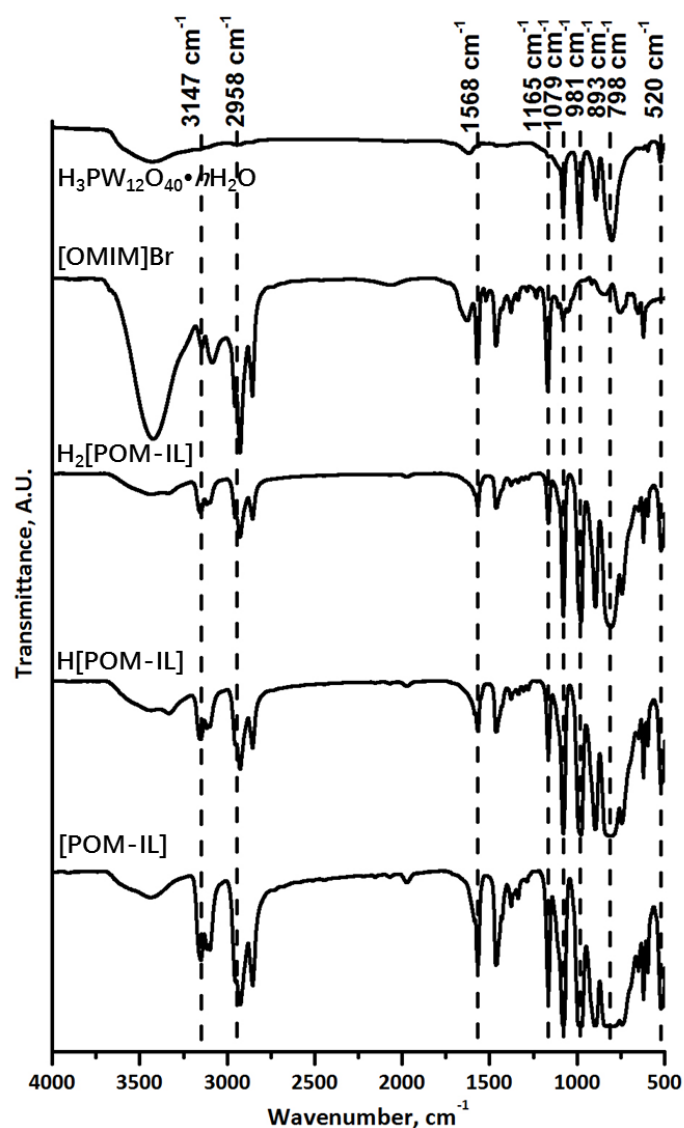
<sup>a</sup>The calculation of surface area was based on multipoint BET method and that of pore volume was based on BJH method. The calculation of pore diameter was based on BJH method. <sup>b</sup>The samples were degassed at 120 °C for 24 h prior to N<sub>2</sub> adsorption-desorption analysis.

**Figure S4.** Pore size distribution of pristine SiO<sub>2</sub> substrate**Table S2.** POM-IL and Pd content (wt. %) of synthesized Pd/POM-IL@SiO<sub>2</sub> and Pd/SiO<sub>2</sub>

Sample	POM-IL content (wt. %)	Pd content (wt. %) <sup>[a]</sup>
Pd/H <sub>2</sub> [POM-IL]@SiO <sub>2</sub>	23.5	3.65
Pd/H[POM-IL]@SiO <sub>2</sub>	24.6	3.53
Pd/[POM-IL]@SiO <sub>2</sub>	25.7	3.66
Pd @SiO <sub>2</sub>	0	3.58

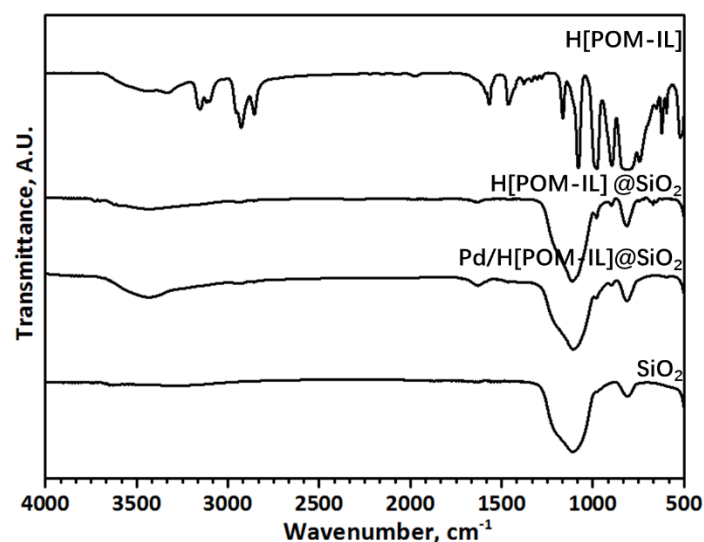
<sup>a</sup>Pd content in the synthesized materials was determined by ICP-AES. The samples were acid digested in aqua regia prior to analysis.

## 2.2 FT-IR characterization of POM-IL complexes and synthesized catalysts

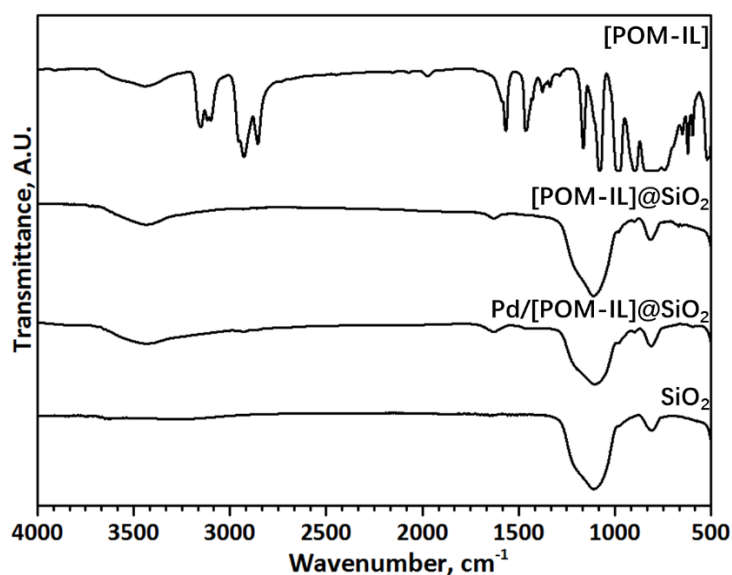


**Figure S5.** FT-IR spectra of  $\text{H}_3\text{PW}_{12}\text{O}_{40} \cdot n\text{H}_2\text{O}$ , [OMIM] Br and synthesized POM-IL complexes.

The FT-IR spectra of  $\text{H}_3\text{PW}_{12}\text{O}_{40} \cdot n\text{H}_2\text{O}$ , [OMIM] Br and synthesized POM-IL complexes (*i.e.*,  $\text{H}_2[\text{POM-IL}]$ ,  $\text{H}[\text{POM-IL}]$  and  $[\text{POM-IL}]$ ) are shown in Figure S5. From the FT-IR spectrum of  $\text{H}_3\text{PW}_{12}\text{O}_{40} \cdot n\text{H}_2\text{O}$ , characteristic bands attributed to the Keggin unit are observed at  $1079\text{ cm}^{-1}$  (P-O band),  $981\text{ cm}^{-1}$  (W-O band),  $893\text{ cm}^{-1}$ , and  $798\text{ cm}^{-1}$  (W-O-W bands) and  $520\text{ cm}^{-1}$  (W-O-P band, weak).<sup>1,2</sup> From the spectrum of [OMIM]Br, characteristic absorption bands attributed to the imidazolium ring are observed at  $3147\text{ cm}^{-1}$ ,  $2958\text{ cm}^{-1}$ ,  $1568\text{ cm}^{-1}$  and  $1165\text{ cm}^{-1}$ , wherein the two bands centered at  $1568\text{ cm}^{-1}$  and  $1165\text{ cm}^{-1}$  are assigned to the  $\text{-C=N-}$  and stretching vibration of the imidazole ring, respectively.<sup>1</sup> The C-H stretching and vibration bands of the imidazole ring and substituent alkyl groups are in the range from  $2990\text{ cm}^{-1}$  to  $2790\text{ cm}^{-1}$  in the spectra of [OMIM]Br and POM-IL complexes. All these major characteristic absorption bands still present in the spectra of synthesized POM-IL complexes, indicating that the structure of anion of phosphotungstic acid and imidazolium group remain intact in general.



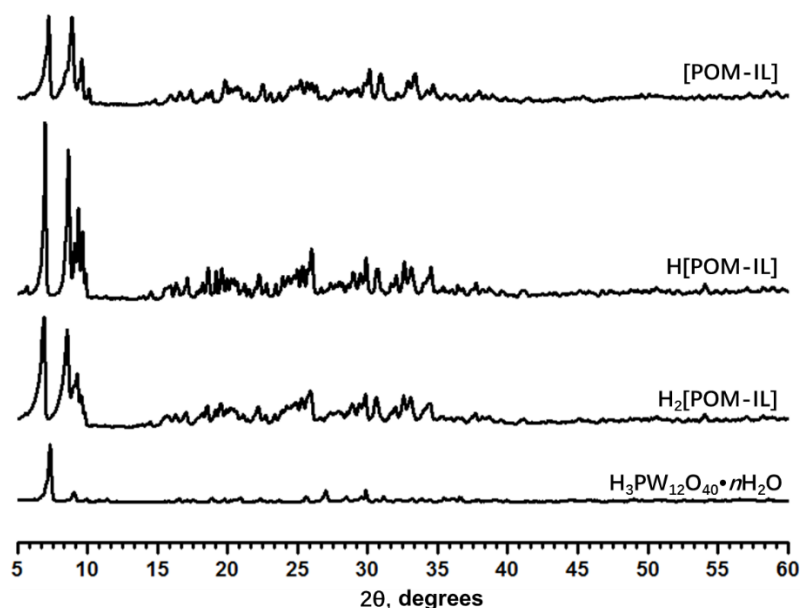
**Figure S6.** FT-IR spectra of H[POM-IL], H[POM-IL]@SiO<sub>2</sub>, Pd/H[POM-IL]@SiO<sub>2</sub> and SiO<sub>2</sub>.



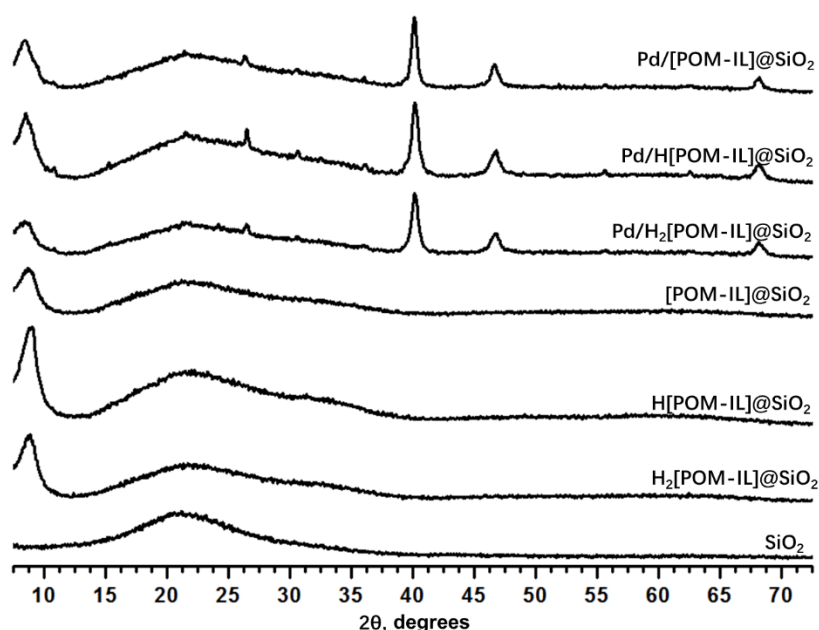
**Figure S7.** FT-IR spectra of [POM-IL], [POM-IL]@SiO<sub>2</sub>, Pd/[POM-IL]@SiO<sub>2</sub> and SiO<sub>2</sub>.

Figure S6 and S7 shows the FT-IR spectra of POM-IL, POM-IL@SiO<sub>2</sub>, and Pd/POM-IL@SiO<sub>2</sub> for H[POM-IL] and [POM-IL], respectively. Those for H<sub>2</sub>[POM-IL] are shown in the main article. For reference, the spectrum of SiO<sub>2</sub> is also shown in these figures. It is obvious that after loading of the POM-IL and Pd NPs onto silica support, the basic structures of imidazolium ring and Keggin units remains. Although many characteristic absorption bands are overlapped by the broad absorption band attributed to SiO<sub>2</sub> ranging from 1315 cm<sup>-1</sup> to 990 cm<sup>-1</sup>, some other absorption bands are still visible in the spectra of POM-IL@SiO<sub>2</sub> and Pd/POM-IL@SiO<sub>2</sub>. For assignments of these bands, please refer to the above discussions.

### 2.3 XRD characterization of POM-IL complexes and synthesized catalysts



**Figure S8.** XRD patterns of H<sub>3</sub>PW<sub>12</sub>O<sub>40</sub>·nH<sub>2</sub>O and POM-IL complexes.



**Figure S9.** XRD patterns of POM-IL@SiO<sub>2</sub> and Pd/POM-IL@SiO<sub>2</sub>.

Figure S8 highlights the XRD patterns of H<sub>3</sub>PW<sub>12</sub>O<sub>40</sub>·nH<sub>2</sub>O and POM-IL complexes (*i.e.*, H<sub>2</sub>[POM-IL], H[POM-IL] and [POM-IL]). Notably, the diffraction patterns of POM-IL complexes are significantly different from that of H<sub>3</sub>PW<sub>12</sub>O<sub>40</sub>·nH<sub>2</sub>O in 5-13°. This is primarily attributed to the substitution of protons in H<sub>3</sub>PW<sub>12</sub>O<sub>40</sub>·nH<sub>2</sub>O by [OMIM] cations. Upon the introduction of [OMIM] Br, the PW<sub>12</sub>O<sub>40</sub><sup>3-</sup> anions reordered with the [OMIM] cations filling the interstitials. Hence, the diffraction bands in this region are resulting from the low-index planes of the generated crystals as the lattice parameters are generally larger than 10 Å.<sup>1</sup> All these samples show long-range order diffraction, owing to the excellent scattering properties of W. The bands ranging from 15° to 45° are resulted from higher index planes of the samples. The major characteristic



diffraction bands of  $\text{H}_3\text{PW}_{12}\text{O}_{40} \cdot n\text{H}_2\text{O}$  are still present in that of POM-IL complexes. These data are in good consistency with the FT-IR characterization results that the major structures (anion from phosphotungstic acid and cation from IL) still exist in the three POM-IL complexes.

Figure S9 compares the XRD patterns of  $\text{POM-IL@SiO}_2$  and  $\text{Pd/POM-IL@SiO}_2$ . For reference, that of  $\text{SiO}_2$  is also presented in this figure. In the diffraction patterns of  $\text{Pd/POM-IL@SiO}_2$ , characteristic diffraction bands of  $\text{Pd}(111)$ ,  $\text{Pd}(200)$  and  $\text{Pd}(220)$  are observed at around  $2\theta=40.1^\circ$ ,  $46.6^\circ$  and  $68.1^\circ$ , respectively.

## 2.4 XPS characterization of Pd in synthesized catalysts

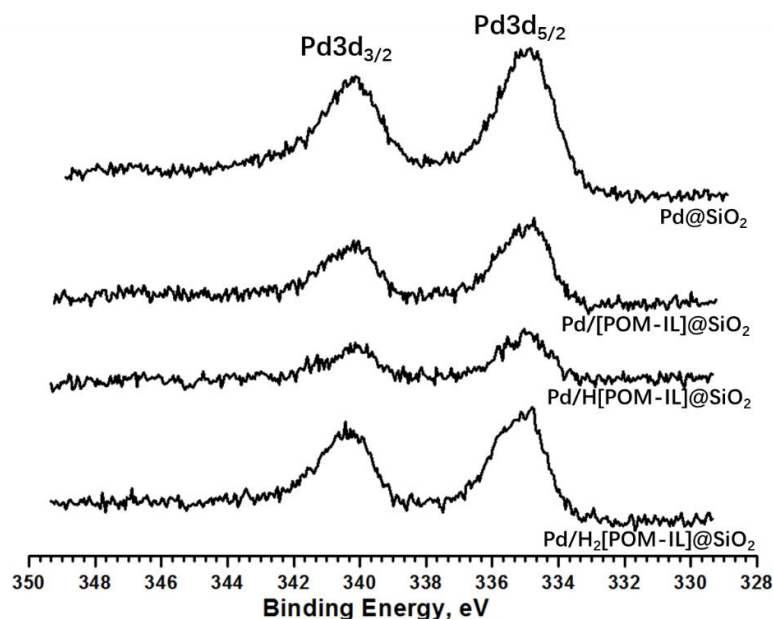


**Figure S10.** XPS spectra of  $\text{Pd}_{3d}$  in  $\text{Pd/POM-IL@SiO}_2$  and  $\text{Pd@SiO}_2$ .

From the XPS spectra of Pd 3d (Figure S10), the  $\text{Pd}_{3d3/2}$  and  $\text{Pd}_{3d5/2}$  bands are centered around 340.4 eV and 335.1 eV, respectively. These results suggest that the substrate to which Pd NPs are loaded on have no significant impact on resulting Pd NPs.

## 2.5 Elemental Mapping Images

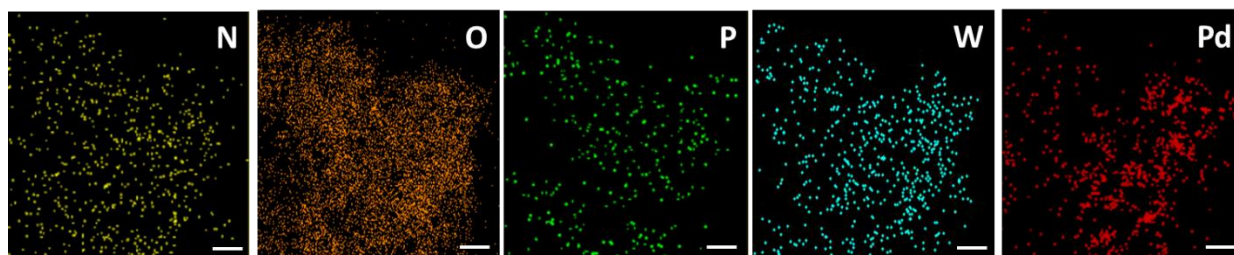
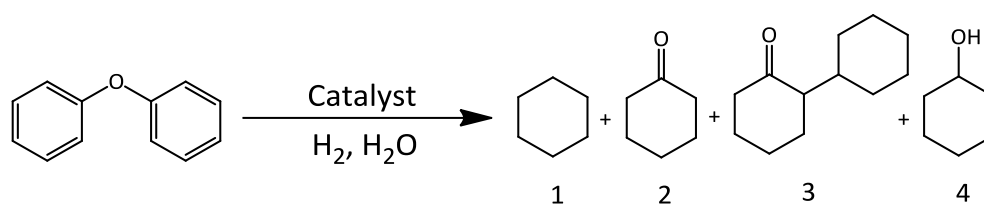


**Figure S11.** Elemental mapping images of  $\text{Pd/H}_2[\text{POM-IL}]\text{@SiO}_2$ , the scale bar is 100 nm.

## 2.6 Additional experiments

**Table S3.** Control experiments: reactions of diphenyl ether over various catalysts<sup>[a]</sup>



Entry	Catalyst	Con. <sup>[b]</sup> (%)	Product distribution and yield (%) <sup>[c]</sup>			
			1	2	3	4
1	None	0	0	0	0	0
2	H <sub>2</sub> [POM-IL]@SiO <sub>2</sub>	0	0	0	0	0
3	H[POM-IL]@SiO <sub>2</sub>	0	0	0	0	0
4	[POM-IL]@SiO <sub>2</sub>	0	0	0	0	0

<sup>a</sup>Reaction conditions: Catalyst, 30 mg; DPE, 1 mmol; H<sub>2</sub>O, 2 mL; H<sub>2</sub>, 3 MPa; temperature, 190 °C; time, 3 h;

<sup>b</sup>Con.: conversion; <sup>c</sup>Conversion and yields are determined by GC using *n*-dodecane as internal standard.

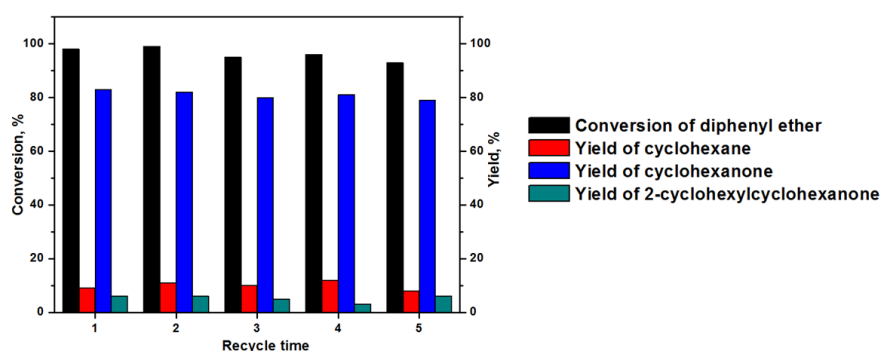


**Figure S12.** Reusability of Pd/H<sub>2</sub>[POM-IL]@SiO<sub>2</sub>. Reaction conditions: DPE, 1 mmol; H<sub>2</sub>, 3 MPa; H<sub>2</sub>O, 2 mL; catalyst, 30 mg; temperature, 190 °C; time, 3 h.

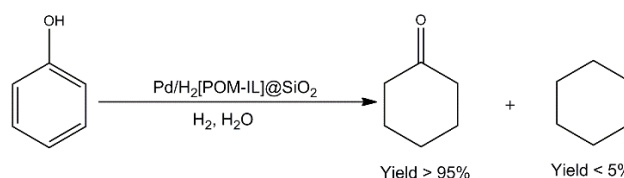


**Figure S13.** Reaction of phenol over Pd/H<sub>2</sub>[POM-IL]@SiO<sub>2</sub>. Reaction conditions: phenol, 1 mmol; H<sub>2</sub>, 3 MPa; H<sub>2</sub>O, 2 mL; catalyst, 30 mg; temperature, 190 °C; time, 1.5 h.

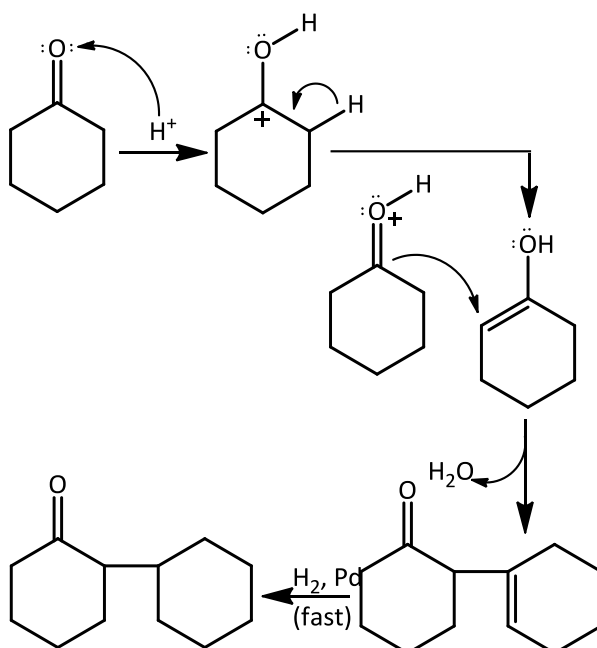


**Figure S14.** Mechanism of aldol-condensation reaction of cyclohexanone for the generation of 2-cyclohexylcyclohexanone. This well-known reaction has been extensively reported in the literature.<sup>3-6</sup>

## References

- (1) X. Xie, J. Han, H. Wang, X. Zhu, X. Liu, Y. Niu, Z. Song and Q. Ge, *Catal. Today*, 2014, **233**, 70.
- (2) C. Pazé, S. Bordiga and A. Zecchina, *Langmuir*, 2000, **16**, 8139
- (3) F. Alvarez, A. I. Silva, F. R. Ribeiro, G. Giannetto, M. Guisnet, In *Studies in Surface Science and Catalysis*; H. U. Blaser, A. Baiker, R. Prins, Eds.; Elsevier, 1997; Vol. 108.
- (4) M. Saidi, P. Rostami, M. R. Rahimpour, B. C. Gates and S. Raeissi, *Energy Fuels*, 2015, **29**, 191.
- (5) J. M. Becker, P. J. Chul, L. O. Winstrom, *US Patents*, US3246036 (1966).
- (6) M. Wan, D. Liang, L. Wang, X. Zhang, D. Yang and G. Li, *J. Catal.*, 2018, **361**, 186.